

Nanoparticle Formation in Water-in-Oil Microemulsions: Experiments, Mechanism, and Monte Carlo Simulation

Mani Ethayaraja, Kanchan Dutta, Devarajan Muthukumar, and Rajdip Bandyopadhyaya*

Department of Chemical Engineering, Indian Institute of Technology Kanpur, Kanpur 208016, India

Received October 3, 2006. In Final Form: January 1, 2007

The dynamics of nanoparticle formation in water-in-oil microemulsions via temporal size evolution has been followed from UV–visible absorption spectra of CdS nanoparticles. Existing Monte Carlo (MC) simulations of nanoparticle formation are primarily based on the mechanism of nuclei formation and their growth by coalescence-exchange of drops, which alone do not predict particles of large size as observed in some experiments. Hence, we have included an additional size enlargement process, namely coagulation of nanoparticles during drop coalescence. We find that particle coagulation, constrained by microemulsion drop size, shows very good agreement with our experimental data on CdS nanoparticle size evolution, for different drop sizes. Thus a combined approach of spectroscopy and MC simulation is helpful in elucidating the mechanism of nanoparticle formation in these confined systems, leading to prediction of size-controlled nanoparticle synthesis.

1. Introduction

Nanoparticles display physical properties different from those of the bulk state of the material.¹ The former possess novel optical, electronic, mechanical, and magnetic properties due to altered electronic structures.² Synthesis of nanoparticles in self-assembled surfactant templates, such as water-in-oil microemulsions, can yield particles nearly monodisperse in size.³ In addition, variation in the water drop size of the microemulsion system gives nanoparticles of controlled mean size. Hence the aforementioned size-dependent properties are accessible by simple control of particle size. These microemulsions are a thermodynamically stable dispersion of nanometer-sized water drops in a continuous oil medium.³ The stability of these drops is attributed to the presence of adsorbed surfactant molecules at the oil–water interface of the drop. The drops undergo Brownian motion, thus colliding with each other and occasionally coalescing. Reactants predissolved in the water drops undergo chemical reaction in this process. Subsequently, the insoluble reaction product nucleates to form a nanoparticle inside the drop.

Despite the availability of a large amount of experimental data on size and size distribution of nanoparticles of various materials (metals, semiconductors, metal oxides, pharmaceutical compounds, etc.), the quest for universal and accurate models for the synthesis process is still on. To understand the mechanism of nanoparticle formation, Monte Carlo (MC) simulation schemes have been developed. The MC scheme of Bandyopadhyaya et al.⁴ is sufficiently general and flexible, and it improved upon the limitations in the earlier work by Li and Park.⁵ The former authors predicted the experimental CdS nanoparticle size of Lianos and Thomas⁶ from MC calculations. They identified coalescence-exchange of drops and nucleation of nanoparticles⁴ to be the most important steps in determining particle size in water-in-oil microemulsions. Coalescence-exchange leads to particle growth,

by bringing into contact a nucleated drop with another drop having only product molecules (nonnucleated). However, it also reduces the chance of nucleation by reducing supersaturation in a drop upon redistributing the product molecules into the two daughter droplets. Nucleation, on the other hand, results in the formation of new particles and reduces the chance of coalescence-exchange-led growth by reducing the number of nonnucleated drops. However, this mechanism,⁴ in some cases, we find underpredicts the final nanoparticle size. This suggests that there must be some other phenomenon playing a pivotal role in nanoparticle growth, in addition to coalescence-exchange-driven growth.

In the simulation scheme of Bandyopadhyaya et al.,⁴ although nucleation and coalescence-exchange were taken into account, particle coagulation during coalescence-exchange was not considered explicitly. Based on measured CdS nanoparticle size, Sato et al.⁷ identified the importance of coagulation of nanoparticles between two nucleated drops. However, their model did not consider the important steps of exchange of reactant and product molecules, nucleation of product, etc. These steps are very important because the relative rates of these strongly affect the size and number of nanoparticles formed. Also, the authors⁷ considered multiple nanoparticles in a single drop, which is not justified from time scale analysis.⁸ In two recent papers, Jain et al.⁹ and Shukla and Mehra¹⁰ reported MC simulation results incorporating coagulation of nanoparticles, first with a constant and then with a size-dependent empirical coagulation rate kernel. The latter work gave a better fit to the single experimental data of Hirai et al.¹¹ used for model discrimination. However, that was due to additional adjustable parameters in the size-dependent empirical coagulation rate kernel, the need and form of the expression of which were not physically justified.

In the present work, we have explored the temporal evolution of CdS nanoparticle size for different microemulsion drop sizes, from both our UV–visible absorption spectra measurements and

* To whom correspondence should be addressed. Telephone: 91-512-259 7697. Fax: 91-512-259 0104. E-mail: rajdip@iitk.ac.in.

(1) Alivisatos, A. P. *J. Phys. Chem.* **1996**, *100*, 13226–13239.
(2) El-Sayed, M. A. *Acc. Chem. Res.* **2004**, *37*, 326–333.
(3) Pileni, M. P. *Langmuir* **1997**, *13*, 3266–3276.
(4) Bandyopadhyaya, R.; Kumar, R.; Gandhi, K. S. *Langmuir* **2000**, *16*, 7139–7149.
(5) Li, Y.; Park, C. W. *Langmuir* **1999**, *15*, 952–956.
(6) Lianos, P.; Thomas, J. K. *Chem. Phys. Lett.* **1986**, *125*, 299–302.

(7) Sato, H.; Asaji, N.; Komasa, I. *Ind. Eng. Chem. Res.* **2000**, *39*, 328–334.

(8) Bandyopadhyaya, R.; Kumar, R.; Gandhi, K. S.; Ramkrishna, D. *Langmuir* **1997**, *13*, 3610–3620.

(9) Jain, R.; Shukla, D.; Mehra, A. *Langmuir* **2005**, *21*, 11528–11533.

(10) Shukla, D.; Mehra, A. *Nanotechnology* **2006**, *17*, 261–267.

(11) Hirai, T.; Sato, H.; Komasa, I. *Ind. Eng. Chem. Res.* **1994**, *33*, 3262–3266.

MC simulation, which are compared against each other. This will help us understand the growth dynamics of nanoparticles for different microemulsion drop sizes. The latter is the single most important and widely employed parameter in different experiments to control particle size. The combined approach of experimental and simulation study will therefore elucidate the mechanism of nanoparticle formation and explain how much drop size can be manipulated to synthesize CdS nanoparticles of controlled size.

2. Experimental Section

2.1. Synthesis of CdS Nanoparticles. AOT [sodium bis(2-ethylhexyl) sulfosuccinate] surfactant (99% pure) and isooctane (2,2,4-trimethylpentane) (99% pure) were purchased from Sigma and Qualigens, respectively. Cadmium nitrate (99% pure) and sodium sulfide (55% pure) were purchased from Merck. These reagents were used as received. Deionized Millipore Milli-Q water was used in all the experiments. A stock solution of 0.1 M AOT in isooctane was prepared. Different water-in-oil microemulsion solutions containing predissolved Cd(NO₃)₂ were prepared by adding requisite amount of aqueous Cd(NO₃)₂ solution to the AOT stock solution, such that the overall Cd(NO₃)₂ concentration with respect to the total dispersion volume was maintained at 1.8×10^{-3} M. Molar ratio (*R*) of water to AOT was varied from 2 to 15. Similar water-in-oil microemulsion solutions with predissolved Na₂S were also prepared. Microemulsion solution without any salt, but of appropriate *R*, was used as a reference for UV–visible absorption measurements. All microemulsions were sonicated for 20 min before mixing and reaction, to ensure that the nanoparticle dispersion, once made, was stable for at least 1 day. Nanoparticle dispersions in microemulsion drops can form loose flocculates due to attractive intermolecular interactions such as van der Waals and electrostatic. It is in this regard that sonication breaks up or prevents such loose flocculates, which otherwise can grow over a period of a few hours or days to cause settling. We also confirmed that nanoparticle size did not change with or without sonication. Hence, the only role of sonication is to increase the stability of the nanoparticle dispersion.

When equal volumes of microemulsions containing Cd(NO₃)₂ and Na₂S were mixed in a cuvette, a deep yellow color instantaneously appeared, confirming the formation of CdS nanoparticles. In situ UV–visible absorption spectra were monitored as a function of time in a UV–visible spectrophotometer (Elico SL159). In subsequent experiments, *R* was varied to study its effect on the control of nanoparticle size, keeping the initial concentrations of all the reactants fixed at 1.8×10^{-3} M with respect to the total microemulsion solution. All the experiments were done at a room temperature of 28 °C.

2.2. Calculation of Nanoparticle Size from UV–Visible Spectra. The UV–visible absorption spectrum of semiconductor nanoparticles is dependent on particle size; using which one can therefore calculate mean nanoparticle size. For this, first the size-dependent band gap energy of semiconductor nanoparticles (E_g) is calculated by fitting the following equation.¹²

$$(\sigma hv)^2 = k(hv - E_g) \quad (1)$$

In eq 1, σ is the molar absorption coefficient, which is obtained from the measured absorption spectra using the Beer–Lambert law, hv is the photon energy, and k is a proportionality factor. A plot of $(\sigma hv)^2$ versus hv shows an intermediate linear region (as given by eq 1), from which one calculates E_g by data fitting. Further, E_g is related to nanoparticle size by an electron–hole-in-a-box model with effective mass approximation according to the following equation.¹³

$$E_g = E_{gb} + \frac{h^2}{2d_p^2} \left(\frac{1}{m_e} + \frac{1}{m_h} \right) - \frac{3.6e^2}{4\pi\epsilon d_p} \quad (2)$$

In eq 2, E_{gb} is the band gap energy of the bulk semiconductor, d_p is the diameter of a nanoparticle, m_e and m_h are the effective masses of electron and hole, e is the electron charge, and ϵ is the dielectric constant of a nanoparticle. For CdS nanoparticles, the values of m_e , m_h , E_{gb} , and ϵ are $0.19m_0$, $0.8m_0$, 2.5 eV, and $5.7\epsilon_0$, respectively.¹¹ Here, m_0 and ϵ_0 are the free electron mass and permittivity of vacuum. Equation 2 has been widely used for the calculation of the size of nanoparticles of CdS, ZnS, AgI, AgBr, etc.^{11,14} Therefore, we have used this model (eq 2) throughout our calculations. However, as an exception, PbS nanoparticles do not obey eq 2, because of its large dielectric constant ($\epsilon = 17.2$) and small effective masses of holes and electrons. Thus a modified form of the effective mass approximation model has been discussed elsewhere for PbS.^{12,15}

3. Mechanism of Nanoparticle Formation

The main features in the mechanism of nanoparticle formation have already been identified on the basis of detailed time scale analysis for various synthetic methods employing water-in-oil microemulsions.^{16–18} Therefore, the mechanism is only briefly presented here. Coalescence of drops, reaction, and exchange of reactant and product molecules after redispersion are shown as the first sequence in Figure 1. It is known that most ionic reactions are very fast compared to the lifetime of a dimer (not shown in Figure 1); hence, the liquid-phase product molecules [C(*l*)], are formed in the dimer itself.¹⁶ Therefore, when the dimer redisperses, both excess reactant and newly formed product molecules are redistributed into the two daughter drops. Nucleation of the nanoparticle [C(*s*)] from the liquid-phase product [C(*l*)] is shown in the second sequence in Figure 1. Growth of the nanoparticle by further liquid product molecules is mediated by coalescence–exchange of drops and is shown next. Finally, coagulation of two nanoparticles during coalescence of the two nucleated drops (bearing these nanoparticles respectively) is an important size enlargement mechanism shown in Figure 1. However, coagulation is constrained by the fact that the coagulated nanoparticle size cannot exceed the size of an individual drop. This is based on the fact that, when a growing nanoparticle approaches the diameter of a microemulsion drop, the head groups of surfactant molecules surrounding the drop can physically adsorb on the nanoparticle surface. Thus, the nanoparticle can become strongly encapsulated in the drop, in comparison to when the particle diameter is much less than the drop diameter. Therefore, we hypothesize that particles of diameter equal to the drop diameter cannot coagulate further with any other nanoparticle.

Sato et al.⁷ have also given a similar explanation for the experimentally observed decrease in coagulation rate, when the nanoparticle diameter approached that of the microemulsion drop. In addition, other experimental studies^{19,20} have also confirmed the adsorption behavior of surfactant molecules on the nanoparticle surface.

(14) Sato, H.; Hirai, T.; Komasa, I. *J. Chem. Eng. Jpn.* **1996**, *29*, 501–507.

(15) Brus, L. *J. Phys. Chem.* **1986**, *90*, 2555–2560.

(16) Bandyopadhyaya, R.; Kumar, R.; Gandhi, K. S. *Langmuir* **2001**, *17*, 1015–1029.

(17) Ethayaraja, M.; Dutta, K.; Bandyopadhyaya, R. *J. Phys. Chem. B* **2006**, *110*, 16471–16481.

(18) Ethayaraja, M.; Bandyopadhyaya, R. *J. Am. Chem. Soc.* **2006**, *128*, 17102–17113.

(19) Mansot, J. L.; Hallouis, M.; Martin, J. M. *Colloids Surf., A* **1993**, *71*, 123–134.

(20) Markovi, I.; Ottewill, R. H.; Cebula, D. J.; Field, I.; Marsh, J. F. *Colloid Polym. Sci.* **1984**, *262*, 648–656.

(12) Wang, Y.; Suna, A.; Mehler, W.; Kasowski, R. *J. Chem. Phys.* **1987**, *87*, 7315–7322.

(13) Brus, L. E. *J. Chem. Phys.* **1984**, *80*, 4403–4409.

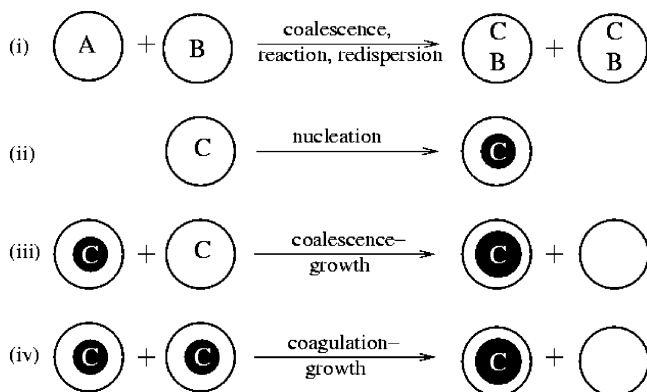


Figure 1. Various elementary events in the formation of nanoparticle (C) with reactants A and B predissolved in two microemulsions. Reactant B is in excess here.

4. Monte Carlo Simulation

Based on the concept of interval of quiescence,²¹ Bandyopadhyaya et al.⁴ have performed Monte Carlo simulations for the prediction of mean and size distribution of nanoparticles synthesized in water-in-oil microemulsion. To this mechanism we now add coagulation of nanoparticles during coalescence-exchange of droplets, if both drops contain a nanoparticle each.

Coalescence-exchange and redispersion of molecules occur in a single step, the total frequency of which over all the drops is given as⁴ $f_c = (1/2)\beta_d q_d N_{\text{drop}} N$, where the collision frequency (q_d) is obtained from the Smoluchowski equation:²²

$$q_d = \frac{8k_B T}{3\eta} \quad (3)$$

Here β_d is the coalescence efficiency, N_{drop} is the number density of drops, k_B is the Boltzmann constant, T is the temperature, and η is the viscosity of oil. Total nucleation frequency is obtained by summing the individual frequencies in each drop as follows:⁴ $f_n = \sum_{j=1}^N k_{n,j}(i)$, where nucleation frequency in the j th drop $k_{n,j}(i)$ is defined as¹⁶

$$k_{n,j}(i) = \begin{cases} 0 & \text{if } i < n^* \\ ik_0 \exp\left(\frac{-16\pi\gamma^3 v_m^2}{3(k_B T)^3 (\ln[\lambda(i)])^2}\right) & \text{if } i \geq n^* \end{cases} \quad (4)$$

In eq 4, k_0 is the preexponential term, n^* is the critical number of CdS molecules required for the formation of a stable nucleus, γ is the interfacial tension between CdS nanoparticle and water, v_m is the volume of one CdS molecule, and λ is the supersaturation of CdS. The total frequency of all the events is $f_t = f_c + f_n$. The interval of quiescence follows an exponential distribution with a mean time equal to the inverse of the total frequency and is given by²¹ $\tau_Q = -\ln(1 - U_1)/f_t$, where U_1 is a uniform random number in $[0, 1)$.

Finally, event selection in MC simulation is based on the probability of occurrence of the i th event, which is given by the respective relative frequency of events, as in $p_i(t) = f_i/f_t(t)$; $i = c$ or n . A uniform random number U_2 in $[0, 1)$ was selected and compared with the cumulative probability of occurrence of events in order to choose an event after a scheduled quiescence interval.

If $U_2 \leq p_c$, coalescence occurs, for which any two drops are randomly selected. If they have reactants A and B, respectively,

Table 1. Parameters Used in Monte Carlo (MC) Simulation

variable	value	reference
$d_{\text{drop}} (R = 2)$	2.8×10^{-9} m	a
$d_{\text{drop}} (R = 6)$	5.45×10^{-9} m	11
$d_{\text{drop}} (R = 10)$	7.07×10^{-9} m	11
$d_{\text{drop}} (R = 15)$	8.32×10^{-9} m	26
k_0	278.42 s^{-1}	4
K_s	$3.6 \times 10^{-29} \text{ mol}^2 \text{ L}^{-2}$	4
N	100 000	optimized
n^*	2	4
$N_{\text{drop}} (R = 2)$	$3.1190 \times 10^{23} \text{ m}^{-3}$	calculated
$N_{\text{drop}} (R = 6)$	$1.2624 \times 10^{23} \text{ m}^{-3}$	calculated
$N_{\text{drop}} (R = 10)$	$9.5552 \times 10^{22} \text{ m}^{-3}$	calculated
$N_{\text{drop}} (R = 15)$	$8.7182 \times 10^{22} \text{ m}^{-3}$	calculated
T	301 K	measured
β_d	10^{-4}	typical value
η	$0.001 \text{ kg m}^{-1} \text{ s}^{-1}$	standard value
γ	0.097 N m^{-1}	4

^a Calculated value of d_{drop} shown for $R = 2$ is obtained by linear interpolation of measured drop size data for the other three R values ($R = 6, 10,$ and 15), which were available in refs 11 and 26.

product molecules $C(l)$ form instantaneously and excess reactant molecules are binomially redistributed over the two daughter drops. If one of the colliding drops has a particle, then the entire $C(l)$ formed leads to particle growth and only the excess reactant is binomially redistributed. However, if both drops have particles, then the two particles coagulate to form a single nanoparticle, and which grows by using all the $C(l)$ molecules available in these two drops. If the final particle size, after coagulation, is bigger than that of an individual drop, then coagulation is not physically possible, but only redispersion of molecules will take place. Drop size, therefore, acts as a constraint to particle size.

Due to nonuniform distribution of $C(l)$ in drops, nucleation rates in each drop can be different. When nucleation is the next due event, the i th drop can nucleate if it satisfies the following criterion.

$$\left(p_c + \frac{\sum_{j=1}^{i-1} k_{n,j}(l,t)}{\sum_{j=1}^N k_{n,j}(l,t)} \right) < U_3 \leq \left(p_c + \frac{\sum_{j=1}^i k_{n,j}(l,t)}{\sum_{j=1}^N k_{n,j}(l,t)} \right) \quad (5)$$

The parameters and constants used in the MC simulation are given in Table 1.

5. Results and Discussion

The inset in Figure 2 shows temporal evolution of UV–visible spectra of CdS nanoparticles corresponding to $R = 6$ (drop size = 5.45 nm), at times $t = 18$ s, 5 min 19 s, and 8 min, respectively. In contrast to the absorption of bulk CdS at 512 nm, the nanosized CdS particles show a peak at 388 nm, at $t = 18$ s. This is due to the quantum confinement effect leading to a blue shift in absorption, compared to the bulk semiconductor. Further, as a function of time, the peak slowly shifts to higher wavelength, which indicates an increase in nanoparticle size. However, beyond 8 min, the absorption characteristics did not change (spectra beyond 8 min are not shown), implying that nanoparticle growth essentially stops. We had also confirmed this with dynamic light scattering (DLS) measurements of CdS nanoparticle diameter. As an example, for the case $R = 6$, a CdS sample was measured (by UV–visible spectroscopy) to have a mean diameter of 5.6 nm at 8 min. A similar sample after 1 day gave 5.0 nm (using DLS). This difference (of 0.6 nm) is within our reported

(21) Shah, B. H.; Ramkrishna, D.; Borwanker, J. D. *AIChE J.* **1977**, *23*, 897–904.

(22) Smoluchowski, M. V. *Phys. Z.* **1916**, *17*, 557.

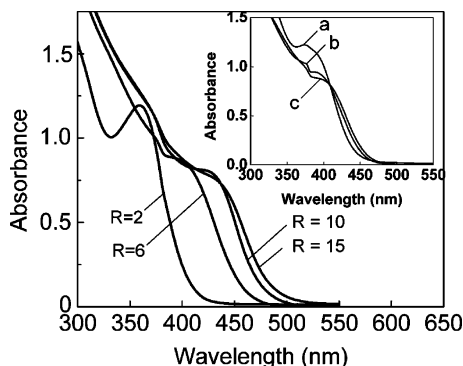


Figure 2. UV-visible spectra of CdS nanoparticles at $t = 8$ min for various R values, synthesized at $[AOT] = 0.1$ M and reactant concentrations of $[Cd(NO_3)_2] = [Na_2S] = 1.8 \times 10^{-3}$ M. Inset shows temporal evolution of UV-visible spectra of CdS nanoparticles synthesized with $R = 6$ and $[Cd(NO_3)_2] = [Na_2S] = 1.8 \times 10^{-3}$ M: (a) 18 s; (b) 5 min 19 s; (c) 8 min.

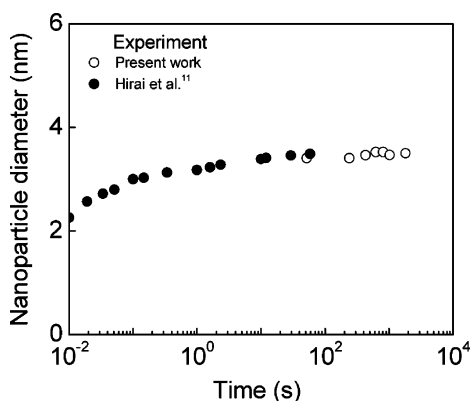


Figure 3. Comparison of temporal evolution of CdS nanoparticle diameter from our experiments (synthesized at $[AOT] = 0.1$ M, $[Cd(NO_3)_2] = [Na_2S] = 1 \times 10^{-4}$ M and $R = 6$), with that of Hirai et al.¹¹

experimental error (± 0.5 nm in Figure 4) and in this case can be even due to the differences in techniques (spectroscopy versus scattering) used for particle size measurement. The CdS nanoparticle suspension was stable for more than 1 day without any perceptible flocculation or settling of particles. Therefore, it can be inferred that nanoparticles do not further coagulate (by the mechanism shown in Figure 1), but reach a maximum size, close to but not exactly equal to the drop size (as will be shown later). This observation confirms our mechanism of particle coagulation being constrained by drop size.

Figure 2 further shows UV-visible absorption spectra of CdS nanoparticles synthesized for increasing R values of 2, 6, 10, and 15, corresponding to increased drop sizes of 2.8, 5.45, 7.07, and 8.32 nm, respectively. For all these cases, concentration of both reactants was kept constant at 1.8×10^{-3} M. These four spectra shown in Figure 2 correspond to that obtained 8 min after instantaneous mixing of two microemulsions containing pre-dissolved $Cd(NO_3)_2$ and Na_2S , respectively. The peak positions in the spectra increase with drop size, which means that nanoparticles of bigger size were formed in larger drops (i.e., systems with higher R).

Figure 3 shows the evolution of nanoparticle diameter (calculated from our UV-visible spectra) as a function of time, for $R = 6$, with both reactant concentrations at 1×10^{-4} M. Our experimental data in Figure 3 are compared with the previously reported temporal evolution of CdS diameter of Hirai et al.,¹¹ who did experiments at the same conditions as ours. These two show good consistency with each other, verifying our experiment

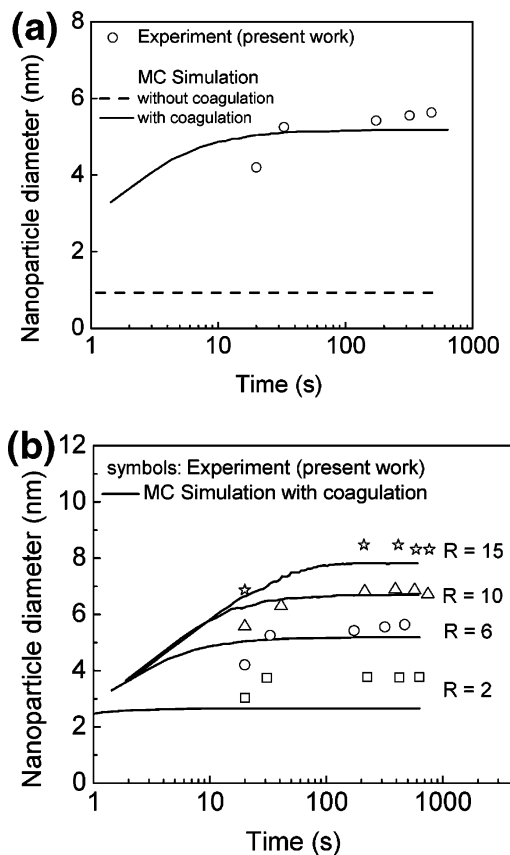


Figure 4. Comparison between our experimental and MC simulation prediction of temporal evolution of CdS nanoparticle diameter, synthesized at $[AOT] = 0.1$ M, $[Cd(NO_3)_2] = [Na_2S] = 1.8 \times 10^{-3}$ M. (a) Importance of particle coagulation, shown for $R = 6$. (b) Experiment compared with MC simulation (with coagulation) for various R values. Description of symbols: (—) MC simulation; (\square) $R = 2$; (\circ) $R = 6$; (\triangle) $R = 10$; (\star) $R = 15$. Experimental error in nanoparticle diameter is approximately ± 0.5 nm, observed from at least three repeated experiments for each data point.

and analysis techniques. Although Hirai et al. are able to measure spectra and therefore calculate particle size at much shorter times than we are, the final size obtained from both experiments is the same.

In Figure 4 we compare our experimental data of CdS nanoparticle diameter with Monte Carlo simulation results. In the absence of particle coagulation (Figure 4a), MC simulation predicts a much smaller nanoparticle diameter than experiments, with the latter being predicted well on including coagulation. This trend was observed for all R values, a representative case ($R = 6$) among which is shown in Figure 4a. Without coagulation, the simulated particle size increased merely within the range of 1–2 nm, as R increased from 2 to 15. However, one can clearly observe (Figure 4b) that the experimentally obtained size is significantly more and increases with R even beyond 8 nm for $R = 15$, thus necessitating the need for including particle coagulation. The latter is part of the new MC scheme of concern to this paper.

From the experimental data (Figure 4b), it can be seen that the final nanoparticle size increases (from 3.7 to 8.3 nm) with increase in R (from 2 to 15). Increase in R , in turn, is known to increase microemulsion drop size. Therefore, R is considered a simple and useful control variable to a priori decide and prepare nanoparticles of desired size. In general, predictions from simulation are in very good agreement with all the experimental runs, except for the case $R = 2$. For $R = 2$, the experimental nanoparticle size (3.7 nm) is higher than the drop size (2.8 nm).

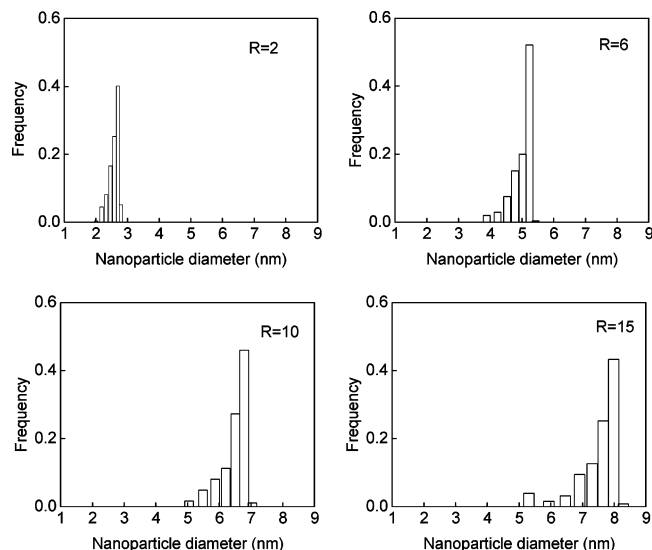


Figure 5. CdS nanoparticle size distribution from MC simulation (with coagulation) for various R values at time $t = 8$ min, synthesized at $[AOT] = 0.1$ M, $[Cd(NO_3)_2] = [Na_2S] = 1.8 \times 10^{-3}$ M.

In this case, simulation gives 2.8 nm, and hence underpredicts compared to experiments. This is due to the different nature of water for very low values of R , since under these conditions the water present in the core of the microemulsion drop has a strong confined nature. It is influenced by the polarity of the ionic head groups of the surfactant molecules, and is known to be different in property from bulk water.^{23–25}

Therefore, based on the above discussion and comparing Figure 4a and Figure 4b, we find that our MC simulation, only on including particle–particle coagulation, shows much better agreement with experiments. Hence, this finding extends our understanding of nanoparticle formation in water-in-oil microemulsions.

Figure 5 shows the final ($t = 8$ min) size distribution of nanoparticles with increasing drop size, as predicted from simulation. When the nanoparticle size approaches that of the drop size, its tendency to coagulate with another nanoparticle diminishes, since the drop size acts as a constraint to coagulation. Thus, the mean nanoparticle size is always slightly less than the corresponding drop size. Hence the particle size distribution is also skewed, with a tail in the lower sizes and the mode near the drop size.

6. Conclusions

Size-controlled CdS nanoparticles have been synthesized in water-in-oil microemulsions of various drop sizes by changing the water to surfactant molar ratio (R). The growth dynamics of CdS nanoparticles were obtained from their UV–visible absorption spectra. The temporal size evolution from these measurements shows strong evidence for growth via coagulation of nanoparticles; this is a new growth mechanism, in addition to that of coalescence-growth used earlier.⁴

Collisions between nucleated microemulsion drops, which were treated as negligible events in most of the previous models, can however be significant. They promote particle growth toward the later stages of the nanoparticle formation process. In contrast, when nucleation is dominant during the initial stages of particle formation, growth by coalescence-exchange is the only growth

mechanism. However, in later stages, when the number of nanoparticles becomes sufficiently large, coagulation of particles during coalescence of drops becomes more important and primarily determines the final nanoparticle size. Particle coagulation however, is not unrestricted; rather the microemulsion drop size (due to its adsorbed surfactant layer) acts as a physical constraint to the maximum achievable particle size by coagulation. Incorporation of a constrained coagulation step gives a very good prediction of our experimental data on the mean CdS nanoparticle diameter as a function of time and drop size. This is true for all cases ($R = 6$ to 15), except for the case of very small microemulsion drop size ($R = 2$), when the nature of water in the drop is known to be different and can cause deviation. Although experiment and simulation are compared for CdS nanoparticle synthesis, the present Monte Carlo simulation scheme is general and can be useful in the quantitative estimation of nanoparticle formation for other systems as well, for example, in the synthesis of core–shell nanoparticles of CdS–ZnS.²⁷

Acknowledgment. We gratefully acknowledge Prof. Sanjeev Garg, Chemical Engineering Department, IIT Kanpur, for letting us generously use the Elico SL159 UV–visible spectrophotometer.

Glossary

d_{drop}	diameter of microemulsion drop, m
d_p	diameter of nanoparticle, m
e	charge of an electron, 1.602×10^{-19} C
E_g	band gap energy of semiconductor nanoparticle, J
E_{gb}	band gap energy of bulk semiconductor, J
f_c	frequency of coalescence event, s^{-1}
f_n	frequency of nucleation event, s^{-1}
f_t	total frequency of all events, s^{-1}
h	Planck's constant, 6.626×10^{-34} J s
k	proportionality constant in eq 1
k_0	preexponential factor in the nucleation rate expression (eq 4), s^{-1}
k_n	nucleation rate in a drop, s^{-1}
m_e	effective mass of an electron, kg
m_h	effective mass of a hole, kg
k_B	Boltzmann constant, 1.3806×10^{-23} J K ⁻¹
K_s	solubility product of CdS, mol ² L ⁻²
n^*	critical number of molecules required for nucleation
N	total number of drops used in MC simulation
N_{drop}	total number density of drops in experiment, m ⁻³
p_c	probability of coalescence event, s^{-1}
p_n	probability of nucleation event, s^{-1}
q_d	Brownian collision frequency of two drops, m ³ s ⁻¹
R	water to surfactant molar ratio
T	temperature, K
U	uniformly distributed random variable in $[0, 1)$
v_m	volume of one CdS molecule, m ³

(23) Kandori, K.; Kon-No, J.; Kitahara, A. *J. Colloid Interface Sci.* **1988**, *122*, 78–82.

(24) Wong, M.; Thomas, J. K.; Nowak, T. *J. Am. Chem. Soc.* **1977**, *99*, 4730–4736.

(25) Hansen, J. R. *J. Phys. Chem.* **1974**, *78*, 256–261.

(26) Hirai, T.; Sato, H.; Komasa, I. *Ind. Eng. Chem. Res.* **1993**, *32*, 3014–3019.

(27) Ethayaraja, M.; Ravikumar, C.; Muthukumaran, D.; Kanchan, D.; Bandyopadhyaya, R. *J. Phys. Chem. C* **2007**, DOI: 10.1021/jp066066j.

Greek Symbols

ϵ	dielectric constant of bulk semiconductor
β_d	coalescence efficiency of drop-drop collision
λ	supersaturation ratio of CdS(l)
η	viscosity, $\text{kg m}^{-1} \text{s}^{-1}$

γ	CdS-water interfacial tension, N m^{-1}
σ	molar absorption coefficient, $\text{M}^{-1} \text{m}^{-1}$
ν	frequency of UV-visible light, s^{-1}
τ_Q	interval of quiescence, s

LA062896C